Observation of a fused dual-fiber sensor head tips by SEM

Xiaoxu Wang (王晓旭), Junxiu Lin (林钧岫), and Dehe Wang (王德和)

Department of Physics, Dalian University of Technology, Dalian 116024

Received April 11, 2005

The shape and microstructure of the fiber-optic liquid-level sensor head, which was made of two fusion-spliced multimode optical fibers, were experimentally studied by using scanning electron microscope (SEM) technology in order to optimize the performance characteristic of the fiber sensor head. The parabolic profile of the sensor head was found to be better and having length-width ratio from 1.2:1 to 1.3:1. Some other useful possibilities were proposed.

OCIS codes: 060.2370, 060.2300.

Optical fiber based liquid-level detecting system has some distinct advantages, such as electricity passive, inherently spark free, immunity to electromagnetic field, flexibility of shape and volume, possibility of remote sensing, ability of multiplexing and distributed sensing, etc.. Because of these advantages, optical fiber liquid-level sensors are particularly suitable to detecting and controlling the level of flammable or explosive liquids in the processing industry. Various optical fiber liquid-level measuring principles and schemes have been proposed in the past few years[1−8]. For discrete or point liquid-level measuring alone, several shapes of optical fiber liquid-level sensor head have been proposed, developed, and used[3−8]. The sensor head tip made of two fusion-spliced multimode optical fiber is one of the above shapes[7,8]. The optical behaviors of this type fiber sensors strongly depended upon their shape and geometry, therefore this paper was focused on the experimental study of the relationship between the shape and the optical behavior of the sensor head tip by using a high performance scanning electron microscope (SEM). Some useful results were reached, which are helpful to optimizing of the sensor head tip during the construction process.

The sensor head tip was made of two fusion-spliced 62.5/125 μm, multimode gradient-index quartz glass fibers by using a GQR-3 program optical fiber splicer. One of the two fibers was the lead-in fiber and the other one was the lead-out fiber. Figure 1 shows the schematic of the construction process for sensor head tip. In order to obtain the relationship between the shapes of sensor head tips and the modulation depth of the corresponding sensors, a series of sensor head tips with different shapes were made.

The following was the sensor head tip spliced construction process. 1) Two fibers with a length of coating removed and cleaned were placed on the same side of a fusion splicer GQR-3 and parallel to each other. The fibers were then longitudinally fused together over a short length. 2) Another fiber (so-called pulled fiber) was axially fusion-spliced to the end of the two fibers fused in step 1). 3) Using appropriate splicing current and time, which both depended on the fiber parameters, the single (pulled) fiber spliced axially to the two longitudinally spliced fibers was pulled quickly along the fiber axial direction during fusion[7], so as obtain different shapes of sensor head tips. Meanwhile the output signals from the sensor head tips were monitored and measured during the fusion process. These output signals were made intentionally different and each sensor head tip was numbered for the later SEM measurement. 4) In order to remove the internal stress in the spliced region, each sensor head tip was treated using lower discharge currents (12.5—13.5 mA) for a short time after the spliced construction process. In order to know how the fiber core and cladding diameters were microscopically changed during the fusion-spliced process, several samples were prepared and polished for the microstructure measuring.

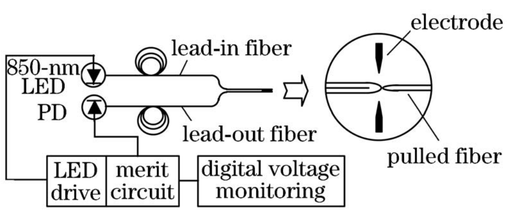

Fig. 1. Schematic of the construction process for sensor head tip.

The fiber-optic liquid-level sensor reported in this paper belongs to the so-called intensity modulated digital optical fiber sensor group. Therefore the sensor's optical characteristic is mainly dependent on its optical modulation depth (OMD) M, which was defined as $M = -10 \lg I_{\rm L}/I_{\rm G}$, where $I_{\rm L}$ is the reflected light power when the sensor head is immersed in water, $I_{\rm G}$ is the reflected light power when the sensor head is exposed in the air. At first the OMDs of some sensor head tips were measured, then the sensor head tips were cut off from the lead-in and lead-out fiber, cleaned and placed into the vacuum chamber of the SEM to be measured and photographed. Three typical shaped-photos of the fusion-spliced sensor head tips, "spindly shape", "circular shape", and "parabolic shape", are shown in Figs. 2(a), (b), and (c), respectively. Their corresponding optical properties were shown in Table 1. It can be evidently seen that the sensor head tip with approximately parabolic shape has the best optical properties of the three typical shapes given in this paper. According to our experiments, the sensor head tips with approximately parabolic shapes and having length-width ratio between 1.2:1—1.3:1 (Fig. 2) have the OMD bigger than 20 dB,

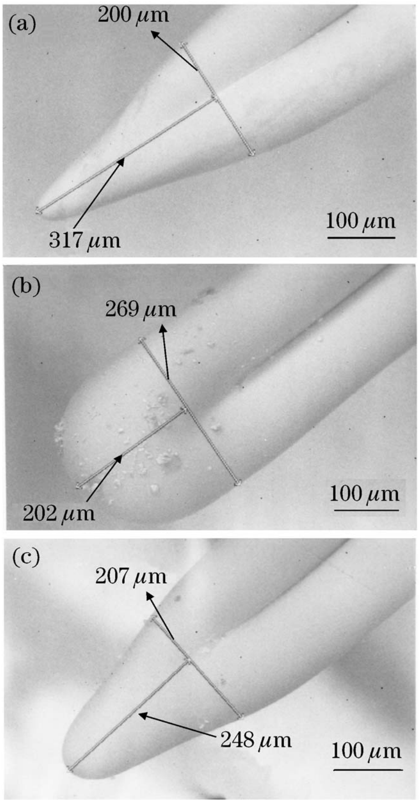

Fig. 2. Three typical shaped-photos of the fusion-spliced sensor head tips by SEM. (a) Spindly; (b) circular; (c) parabolic.

Table 1. Optical Properties of Different Sensor Head Tips. All the Optical Powers Coupled in Fiber are 53.4 μW

Shape	I_G (μW)	I_L (nW)	M (dB)
Spindly	0.536	54.6	9.9
Circular	0	0	—
Parabolic	5.33	52.1	20.1

and they are useful in digital liquid-level fiber sensor system[8].

The refractive index difference between core and cladding of the multimode fiber used in our experiments was 1%, therefore the boundary interface between core and cladding may be visible under SEM. The SEM used in our experiments was the type JEOL JSM-5600LV made in Japan. The working principle of SEM is well known, the secondary electron emission was dependent on the surface structure and ingredients of the samples to be measured. To further investigate the microstructure deformation in the fusion-spliced sensor head tip, several samples were prepared and placed into the vacuum chamber of SEM to be photographed. Three typical photos of this sample series are shown in Fig. 3. The cross section of the multimode fiber before fusing is shown in Fig. 3(a). This photo verified clearly that the boundary interface between core and cladding could be made visible by SEM. The core diameter measured in Fig. 3(a) was not 62.5 μm, but 65.5 μm, because the interface between core and cladding of the gradient-index fiber was not very sharp. After the fusion spliced process, a few

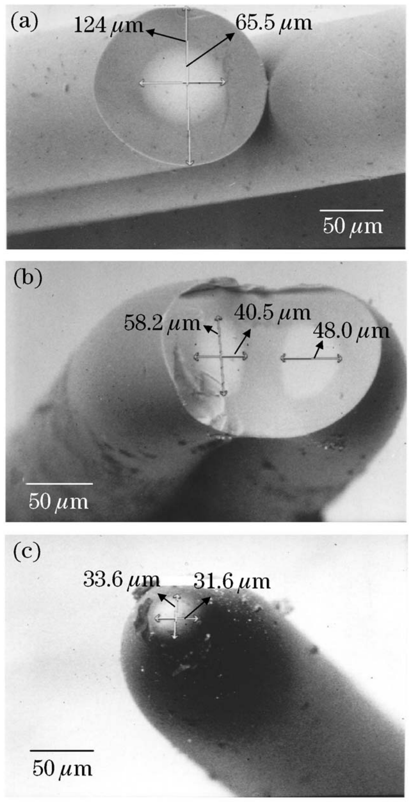

Fig. 3. Three typical photos of fiber microstructure by SEM. (a) Cross section of a fiber, (b) sensor head tip polished to medium, (c) sensor head tip polished at the top.

sensor head tips were cut off and polished to different depth by polishing machine type UT-Ultrapol1200 made in USA in order to know the deformation of core and cladding during the fusion spliced process. Figures 3(b) and (c) show the results. It was distinct to see that the core and cladding of the two multimode fibers were gradually deformed and closed together (Fig. 3(b)), finally fused at the top of the sensor head tip (Fig. 3(c)). The core deformation was the main reason why the total-reflection condition within the fused sensor head tip region at the boundary surface between the core and cladding of the two multimode fibers could not be fulfilled.

Based on the experimental results, we could explain the relationship between the OMD and the shape of the sensor head tips. It was the deformation of the core and cladding of the fiber related to the shape of the spliced region that determines the amount of the reflected power from the sensor head tips. We discussed the condition of the circular and noncircular shape. 1) For the circular shape sensor head tip, the cores of the two fibers had not been fused thoroughly, so its reflected power was zero even if it was bared in air. 2) For the spindly and the parabolic shape sensor head tips, the cores were deformed gradually and fused at the exact tips of the sensor head, so their OMD was not zero; but the spindly shape head tip was too sharp to carry out an optical total-reflection at the tip. It was the reason that its OMD was small compared with that of the parabolic shape head tip. The parabolic shape head tip was not so sharp that made it have a larger fused region where total-reflection condition could be satisfied. Thus, it had a better OMD.

In one word, the shape of the fused dual-fiber sensor head tips should not be too circular or too sharp. Our results show that the optimal length-width ratio is from 1.2:1 to 1.3:1.

In addition, the SEM technology could supply some possible measuring applications for fiber optic and multi-layer thin film optical components, for example: a complementary method to measure the geometrical parameters of optical fibers, such as non-circularity of core and cladding, the core to cladding concentricity etc.. It may be also a good tool to measure and control the quality of multi-layer thin film[9], such as layer-thickness and layer-homogeneity, if the refractive index difference between the layers is enough for the resolution of SEM and the cross section of the multi-layer thin film was suitably prepared.

In conclusion, the relationship between the fusion spliced multimode fiber sensor head tip and the modulation depth M has been studied by using SEM technology and it was found that sensor head tip with approximately parabolic shape and having the length-width ratio between 1.2:1—1.3:1 had the modulation depth bigger than 20 dB. The microstructure deformation of core and cladding in the spliced region has been shown by SEM photos. Some other possible measuring applications of SEM technology in fiber optic and in multi-layer thin film technique have been proposed.

J. Lin is the author to whom the correspondence should be addressed, his e-mail address is jxlin@dlut.edu.cn.

References

1. T. I. Murashkina, Telecommun. Radio Eng. **49,** 46 (1995).
2. G. Betta, L. Ippolito, A. Pietrosanto, and A. Scaglione, IEEE Trans. Instrumentation and Measurement **44,** 686 (1995).
3. P. Raatikainen, I. Kassamakov, R. Kakanakov, and M. Luukkala, Sensors and Actuators A **58,** 93 (1997).
4. G. Betta, A. Pietrosanto, and A. Scaglione, IEEE Trans. Instrumentation and Measurement **45,** 551 (1996).
5. J. Niewisch, Siemens Forsch.-u. Entwickl.-Ber. Bd. **15,** 115 (1986).
6. K. Wamoto and I. Kamata, Appl. Opt. **31,** 51 (1992).
7. A. Wang, M. F. Gunther, K. A. Murphy, and R. O. Claus, Sensors and Actuators A **35,** 161 (1992).
8. J. Lin, X. Yu, X. Wang, and Q. Yu, Laser Opto. **33,** 56 (2001).
9. J. G. N. Baines, A. G. Hallam, K. W. Raine, and N. P. Turner, J. Lightwave Technol. **18,** 1259 (1990).